Photon statistics and polarization correlations at telecommunications wavelengths from a warm atomic ensemble

R. T. Willis,[1] **F. E. Becerra,**[1,2] **L. A. Orozco,**[1,*] **and S. L. Rolston**[1]

[1]*Joint Quantum Institute, Department of Physics, University of Maryland and National Institute of Standards and Technology, College Park, Maryland 20742, USA*
[2]*Departamento de Física, CINVESTAV, Apdo. Post. 14-740, 07000 México, Distrito Federal, México*
[*]*lorozco@umd.edu*

http:www.jqi.umd.edu

Abstract: We present measurements of the polarization correlation and photon statistics of photon pairs that emerge from a laser-pumped warm rubidium vapor cell. The photon pairs occur at 780 nm and 1367 nm and are polarization entangled. We measure the autocorrelation of each of the generated fields as well as the cross-correlation function, and observe a strong violation of the two-beam Cauchy-Schwartz inequality. We evaluate the performance of the system as source of heralded single photons at a telecommunication wavelength. We measure the heralded autocorrelation and see that coincidences are suppressed by a factor of ≈ 20 from a Poissonian source at a generation rate of 1500 s^{-1}, a heralding efficiency of 10%, and a narrow spectral width.

OCIS codes: (270.5290) Photon statistics; (020.4180) Multiphoton processes; (270.5585) Quantum information and processing.

References and links

1. C. H. Bennett and G. Brassard, "Quantum cryptography: public key distribution and coin tossing," in Proceedings of the IEEE International Conference on Computers, Systems and Signal Processing, Bangalore, India (IEEE, 1984), p. 175.
2. A. K. Ekert, "Quantum cryptography based on bell's theorem," Phys. Rev. Lett. **67**, 661–663 (1991).
3. L. Duan, M. Lukin, J. Cirac, and P. Zoller, "Long-distance quantum communication with atomic ensembles and linear optics," Nature **414**, 413–418 (2001).
4. A. Kuzmich, W. P. Bowen, A. D. Booze, A. Boca, C. W. Chou, L.-M. Duan, and H. J. Kimble, "Generation of nonclassical photon pairs for scalable quantum communication with atomic ensembles," Nature **423**, 731–734 (2003).
5. C. H. van der Wal, M. D. Eisaman, A. Andre, R. L. Walsworth, D. F. Phillips, A. S. Zibrov, and M. D. Lukin, "Atomic memory for correlated photon states," Science **301**, 196–200 (2003).
6. V. Balic, D. A. Braje, P. Kolchin, G. Yin, and S. E. Haris, "Generation of paired photons with controllable waveforms," Phys. Rev. Lett. **94**, 183601 (2005).
7. S. Du, P. Kolchin, C. Bethangady, G. Yin, and S. E. Harris, "Subnatural linewidth biphotons with controllable temporal length," Phys. Rev. Lett. **100**, 183603 (2008).
8. T. Chanelière, D. N. Matsukevich, S. D. Jenkins, T. A. B. Kennedy, M. S. Chapman, and A. Kuzmich, "Quantum telecommunication based on atomic cascade transitions," Phys. Rev. Lett. **96**, 093604 (2006).

#148821 - $15.00 USD Received 7 Jun 2011; revised 2 Jul 2011; accepted 3 Jul 2011; published 14 Jul 2011

9. K. F. Rim, J. Nunn, V. O. Lorenz, B. J. Sussman, K. C. Lee, N. K. Langford, D. Jaksch, and I. A. Walmsley, "Towards high-speed optical quantum memories," Nat. Photonics **4**, 218–221 (2010).
10. N. Gisin, G. Ribordy, W. Tittel, and H. Zbinden, "Quantum cryptography," Rev. Mod. Phys. **74**, 145–195 (2002).
11. E. A. Goldschmidt, M. D. Eisaman, J. Fan, S. V. Polyakov, and A. Migdall, "Spectrally bright and broad fiber-based heralded single-photon source," Phys. Rev. A **78**, 013844 (2008).
12. A. R. McMillan, J. Fulconis, M. Halder, C. Xiong, J. G. Rarity, and W. J. Wadsworth, "Narrowband high-fidelity all-fibre source of heralded single photons at 1570 nm," Opt. Express **17**, 6156–6165 (2009).
13. S. Fasel, O. Alibart, S. Tanzilli, P. Baldi, A. Beveratos, N. Gisin, and H. Zbinden, "High-quality asynchronous heralded single-photon source at telecom wavelength," N. J. Phys. **6**, 163 (2004).
14. O. Alibart, D. B. Ostrowsky, P. Baldi, and S. Tanzilli, "High-performance guided-wave asynchronous heralded single-photon source," Opt. Lett. **30**, 1539–1541 (2005).
15. A. G. Radnaev, Y. O. Dudin, R. Zhao, H. H. Jen, S. D. Jenkins, A. Kuzmich, and T. A. B. Kennedy, "A quantum memory with telecom-wavelength conversion," Nat. Phys. **6**, 894–899 (2010).
16. Y. O. Dudin, A. G. Radnaev, R. Zhao, J. Z. Blumoff, T. A. B. Kennedy, and A. Kuzmich, "Entanglement of light-shift compensated atomic spin waves with telecom light," Phys. Rev. Lett. **105**, 260502 (2010).
17. R. T. Willis, F. E. Becerra, L. A. Orozco, and S. L. Rolston, "Four-wave mixing in the diamond configuration in an atomic vapor," Phys. Rev. A **79**, 033814 (2009).
18. F. E. Becerra, R. T. Willis, S. L. Rolston, and L. A. Orozco, "Nondegenerate four-wave mixing in rubidium vapor: the diamond configuration," Phys. Rev. A **78**, 013834 (2008).
19. W. Z. Zhao, J. E. Simsarian, L. A. Orozco, and G. D. Sprouse, "A computer-based digital feedback control of frequency drift of multiple lasers," Rev. Sci. Instrum. **69**, 3737–3740 (1998).
20. R. T. Willis, F. E. Becerra, L. A. Orozco, and S. L. Rolston, "Correlated photon pairs generated from a warm atomic ensemble," Phys. Rev. A **82**, 053842 (2010).
21. J. F. Clauser, M. A. Horne, A. Shimony, and R. A. Holt, "Proposed experiment to test local hidden-varible theories," Phys. Rev. Lett. **23**, 880–884 (1969).
22. H. J. Metcalf and P. Straten, *Laser Cooling and Trapping* (Springer, 1999).
23. Q. Zhou, W. Zhang, J.-R. Cheng, Y.-D. Huang, and J.-D. Peng, "Properties of optical fiber based synchronous heralded single photon sources at 1.5 μm," Phys. Lett. A **375**, 2274–2277 (2011).
24. A. F. Molisch and B. P. Oehry, *Radiation Trapping in Atomic Vapours* (Oxford University Press, 1998).
25. L. Mandel and E. Wolf, *Optical Coherence and Quantum Optics* (Cambridge University Press, 1995).
26. M. D. Reid and D. F. Walls, "Violations of classical inequalities in quantum optics," Phys. Rev. A **34**, 1260–1276 (1986).
27. Q.-F. Chen, B.-S. Shi, M. Feng, Y.-S. Zhang, and G.-C. Guo, "Non-degenerate nonclassical photon pairs in a hot atomic ensemble," Opt. Express **16**, 21708–21713 (2008).

1. Introduction

Sources of entangled photon pairs and heralded single photons (HSP) have applications to quantum information science, quantum cryptography, and to fundamental tests of quantum mechanics. Quantum communication schemes such as the BB84 [1], Ekert protocol [2], and their more advanced offspring often rely on entangled photon pairs and single-photon states. In the last decade, sources that create photons with compatible frequencies and bandwidths for interacting with atomic systems have been a focus of investigation, due to the potential utility of the atomic ensemble-based quantum repeater [3].

Pair production from atomic ensembles is a natural method for creating these atom-compatible photons. The seminal experiments were performed by Kuzmich *et al.* [4] in a cold atomic ensemble and van der Wal *et al.* [5] in a warm atomic system. Work has continued in both cold and warm ensembles [6–9]. Generally these schemes take advantage of the χ_3 nonlinearity in the atomic vapor through a spontaneous four-wave mixing (4WM) or Raman interaction in the atoms. Two pump beams are applied to the atomic medium. When a spontaneously generated idler photon emits into the phase-matched direction, a second signal photon is emitted that is correlated with the idler in time, energy, direction and polarization. This method shares features with spontaneous parametric down conversion (PDC) in non-linear crystals, but the spectrum of the generated photons is much narrower due to resonant enhancement from the near-resonant energy levels in the atoms.

Any source of correlated photon pairs, regardless of the generation medium, can be cast as

#148821 - $15.00 USD Received 7 Jun 2011; revised 2 Jul 2011; accepted 3 Jul 2011; published 14 Jul 2011

a HSP source. In this application a signal photon is first detected, announcing the presence of a correlated single idler photon in the other mode. For quantum communication this type of single photon source has advantages over weak coherent pulses [10]. Experimental work in this field has included generation from microstructure fibers [11, 12], PDC [13], and crystal waveguides [14]. A high quality HSP source should have a high heralding efficiency, high generation rate, and be spectrally narrow, especially if it is to be used to interact with atomic ensembles.

In this paper we present measurements of correlated photon pairs generated by spontaneous 4WM in a warm atomic vapor cell (See Fig. 1A for the geometry of the experiment). An obvious advantage of a warm atom generation medium is its technological simplicity, compared to cold (i.e. laser-cooled) atomic systems, where recent work now includes quantum memories [15,16]. Our photon pairs are generated at 1367 nm, which is a telecommunications wavelength, and 780 nm, which could interface with an atomic quantum memory. We show that the photon pairs are polarization entangled by measuring a violation of Bell's inequality. We evaluate the performance of the system as a source of HSPs, showing a much higher spectral brightness than sources based on PDC. Additionally we measure the cross-correlation function of the generated pairs as well as the autocorrelation of each of the two beams. From these measurements we compare the results to that expected from a classical source through the Cauchy-Schwarz inequality and show that system is strongly non-classical.

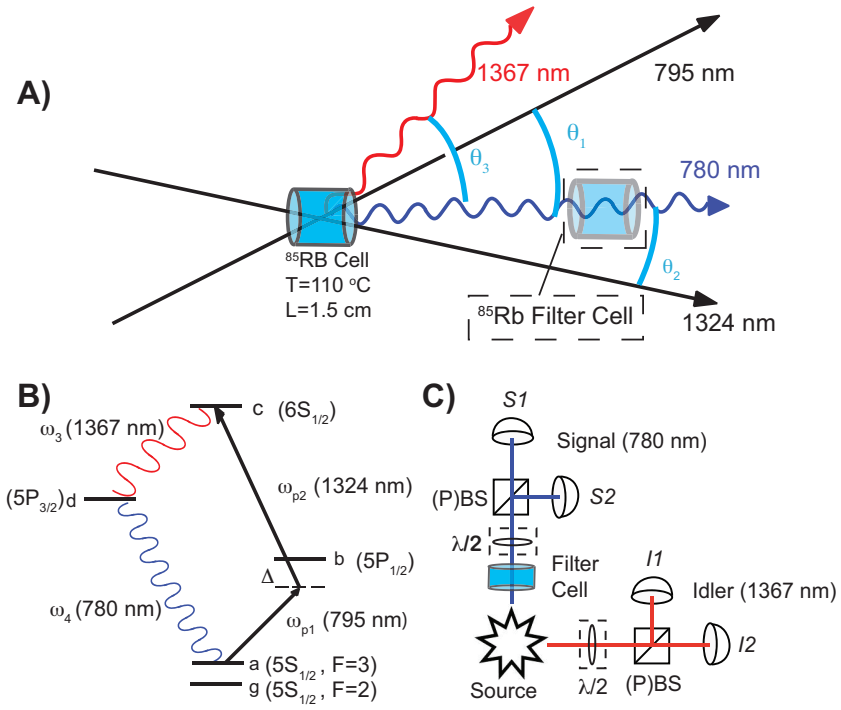

Fig. 1. **A)** The geometry of the experiment: the angles are $\theta_1 = 2^\circ$, $\theta_2 = 0.7^\circ$, and $\theta_3 = 2.7^\circ$. An auxiliary ^{85}Rb filter cell can intersect the 780 nm beam as indicated. **B)** The diamond configuration in ^{85}Rb. **C)** Schematic of detection set up. For polarization correlation measurements the beam splitters (BS) are replaced with polarizing beamsplitters (PBS) and half-wave plates are inserted into each beam path.

#148821 - $15.00 USD Received 7 Jun 2011; revised 2 Jul 2011; accepted 3 Jul 2011; published 14 Jul 2011

2. System

The generation medium is a warm vapor cell of isotopically pure ^{85}Rb atoms which is 1.5 cm long and is maintained at a temperature of 388 K. We utilize the diamond atomic level structure [17, 18] as shown in Fig. 1B. The pump lasers are at 795 nm and 1324 nm with directions defined by $\vec{k}_1$ and $\vec{k}_2$ respectively. The lasers are frequency locked. The 795 nm laser gets its feedback from saturation spectroscopy on an atomic cell [18], while a cavity transfer lock keeps the 1324 nm laser in postion [19].

We observe correlated pairs at 1367 nm and 780 nm with k-vectors $\vec{k}_3$ and $\vec{k}_4$. The phase matching condition, $\vec{k}_1+\vec{k}_2=\vec{k}_3+\vec{k}_4$ determines the direction of the generated pairs and we observe those pairs that appear in the plane defined by the pump beams. We detune the 795-nm pump laser 1.5 GHz below the $5S_{1/2}$ F=3 $\rightarrow$ $5P_{1/2}$ F=2 transition for all the data in this paper; the excitation is outside $D1$ line Doppler width. The 1324-nm laser is tuned so that the pump lasers are two-photon resonant with the $5S_{1/2}$ F=3 $\rightarrow$ $6S_{1/2}$ F=2 transition. The power in the 1324-nm laser is 5 mW. Both pump beams have gaussian profiles and waists of ≈ 1 mm.

Figure 1C shows a schematic of the detection set up. The 780-nm photons are coupled into a short single-mode fiber and then through a fiber-based 50/50 beamsplitter. The two output ports of the beam splitter are coupled to two free-running silicon avalanche photodiodes ($S1$,$S2$) with $\approx 40\%$ detection efficiency. The 1367-nm photons are coupled into a 200-m single mode fiber which serves to optically delay the photons 1 μs. The light is split by a fiber-based 50/50 beamsplitter and then goes to two InGaAs APD detectors ($I1$, $I2$). The InGaAs APDs have detection efficiencies of $\approx 10\%$ and are gated on for 1 ns. The dark count rate is 3×10^{-6} counts per nanosecond gate interval.

A second ^{85}Rb cell (Fig. 1A) is placed in the 780 nm beam path between the generation medium and the fiber coupler. This cell is 5 cm long and held at 320 K. The purpose of second cell is to spectrally filter 780-nm photons that have multiply scattered in the optically thick 4WM cell [20].

3. Polarization correlation

Conservation of energy, linear momentum and angular momentum among the four fields that interact in the 4WM process impose strong correlations among the generated photons, but the quantum nature of the correlation is most readily explored through Bell's inequality. We perform polarization-correlation measurements at zero delay with 15 mW of 795-nm pump power and both pumps horizontally polarized. We fix the polarization analyzer for the 1367-nm photon and measure the coincidence rate as a function of 780-nm polarization analyzer angle and utilize the Clauser, Horne, Shimony and Holt (CHSH) version of Bell's inequality [21] to look for non-classicality and entanglement. Figure 2 shows the coincidence rate as a function of polarization angle with the filter cell in place to reduce the background coincidences resulting in a visibility to $92(2)\%$ We observe clear violation of the CHSH inequality with $S=2.23(3)>2$ without any background subtraction, where the uncertainty is statistical (1-σ). We determine the state to be $|\psi\rangle=(\cos(\Delta\theta)|HH\rangle+\sin(\Delta\theta)|VV\rangle)$ with $\Delta\theta=43.3(6)^\circ$, with a reduced χ^2=1.21 for the fit, disregarding the uncorrelated background. This corresponds closely to the ϕ^+ Bell state. With orthogonal pump polarizations, the generated state is the Ψ^+ Bell state, which is also entangled and violates the CHSH inequality with $S=2.034(4)$. The fringe visibility from a similar measurement to that of Fig. 2 gives $86(5)\%$ for this polarization arrangement. The generation efficiency, however, is about ten times smaller than that with the parallel polarization pump beams.

#148821 - $15.00 USD Received 7 Jun 2011; revised 2 Jul 2011; accepted 3 Jul 2011; published 14 Jul 2011

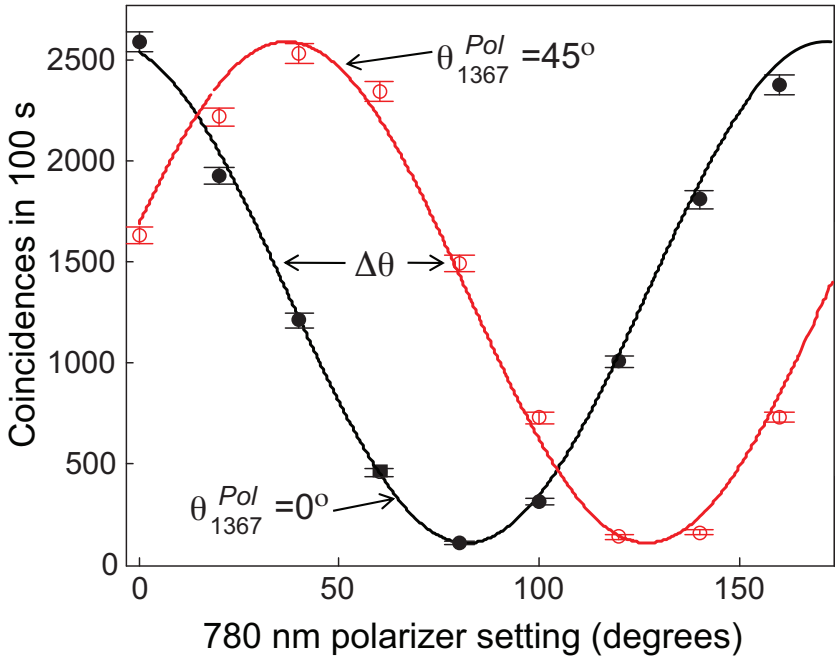

Fig. 2. (Color online) Polarization correlations: Coincidence counts (filled and empty circles) in 100 s as a function of 780 nm polarizer angle for two angles of the 1367 nm polarizer when the pump 795 nm and 1324 nm have parallel polarizations and using the filter cell at 323 K. The experimental data (circles) fit to the function $\cos^2(\Theta_{780} - \Theta_{1367})$ (solid lines). The filter cell reduces the background coincidences and increase the visibility to 92(2)%.

Bell State Calculation

When the two pump polarizations are parallel their polarizations can be taken to be π-polarized by defining the quantization axis along their polarizations. The two-photon pump process $5S_{1/2} \rightarrow 5P_{1/2} \rightarrow 6S_{1/2}$ then does not transfer angular momentum from the pump photons to the atoms. In this case the initial atomic state m_J, the intermediate state $m_{J'}$ and the double excited state $m_{J''}$ (with $J'' = J$) will have the same value describing the process with no angular momentum transfer.

The requirement that the atomic state does not change angular momentum before and after the interaction with the photons in the 4WM process limits the possible polarizations of the generated pairs. After the two-photon excitation with parallel pump beams from the initial level m_J to the level $m_{J''}$, the 4WM process requires a two-photon decay from the level $m_{J''}$ back to the same level m_J. There are different possibilities for the polarization of the photons in this two photon decay process, but they have to satisfy the angular momentum of the atom and this is behind the the entanglement and the generation of the ϕ^+ Bell state .

We next sketch the calculation for the expected polarization state starting with the Hamiltonian of the field interacting with a single atom including all the relevant hyperfine and Zeeman structure, keeping up to the lowest order term in perturbation theory which contributes to the generation of phase matched photons.

We assume a single atom sitting at the origin pumped by two classical monochromatic $\hat{\pi}$ polarized plane wave pump beams with Rabi frequencies Ω_1 and Ω_2 and detunings Δ_1 and Δ_2. The pumps propagate in the $\hat{x}$ direction (see Fig. 3A). The emitted photons are represented by

#148821 - $15.00 USD Received 7 Jun 2011; revised 2 Jul 2011; accepted 3 Jul 2011; published 14 Jul 2011

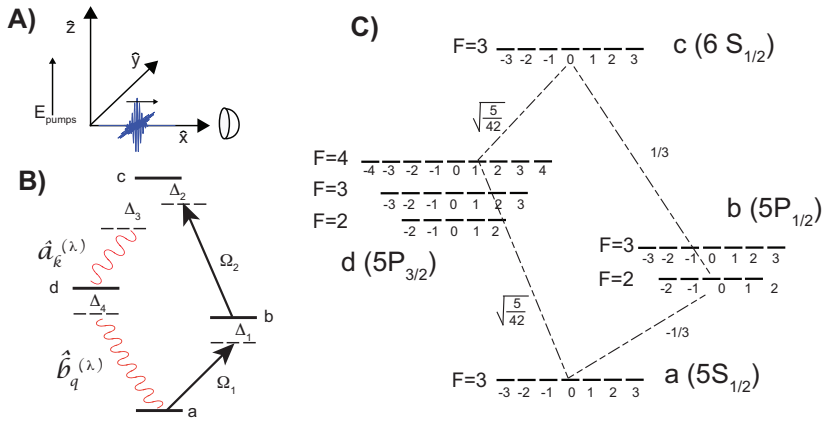

Fig. 3. **A)** Geometry used in the calculation. The pumps are polarized along the z-axis and all fields propagate along the x-axis. **B)** Simplified atomic level structure along with the coupling fields. **C)** Full level atomic structure which is taken into account in the calculation. The dashed lines show an example of a path out of the $m_F = 0$ ground state, along with the Clebsh Gordan weights, that contributes to the 4WM and returns to the same level.

the field operators $\hat{a}_k^{(\lambda)}$ and $\hat{b}_q^{(\lambda)}$, where the λ denotes the two polarization modes, which for the phase matched direction are horizontal $\equiv \hat{z} = \hat{u}_0$ and vertical $\equiv \hat{y} = \frac{i}{\sqrt{2}}(\hat{u}_{+1} + \hat{u}_{-1})$. The operators for the appropriate atomic transitions as labeled in Fig. 3B are $\hat{\sigma}^{ij}$. We follow the conventions of Ref. [22] when it comes to polarization and Clebsch-Gordan coefficients for the dipole couplings g^{ij}. The interaction Hamiltonian in the interaction picture is:

$$\begin{aligned} V_I &= \hbar\sum_{i,j}\Omega_1^{ij}\hat{\sigma}_{ba}^{ij}e^{i\Delta_1^{ij}t} + \hbar\sum_{i,j}\Omega_2^{ij}\hat{\sigma}_{cb}^{ij}e^{i\Delta_2^{ij}t} + \text{H.C.} \\ &\quad + \sum_k\sum_{i,j}{}^{(\lambda)}g_k^{ij}\hat{a}_k^{(\lambda)}\hat{\sigma}_{cd}^{ij}e^{i\Delta_k^{ij}t} + \sum_q\sum_{i,j}{}^{(\lambda)}g_q^{ij}\hat{b}_q^{(\lambda)}\hat{\sigma}_{da}^{ij}e^{i\Delta_q^{ij}t} + \text{H.C.} \end{aligned} \tag{1}$$

The term that corresponds to pair generation comes at fourth order in perturbation theory. We only consider terms that contribute to pairs emitted into the $\hat{x}$ direction. We first take into account only one of the initial Zeeman sub-states, denoted by α. The total wave-function can be written as $|\psi\rangle = |0\,0\,a\rangle + |\psi_{4WM}\rangle + |\psi_{\text{OTHER}}\rangle$. The first term is the vacuum with the atom in the ground state and the result for the 4WM piece is:

$$|\psi_{4WM}\rangle \propto \sum_{k,q}\sum_{\lambda,\gamma}\sum_{j,k,l}\Omega_1^{j\alpha}\Omega_2^{k,j\ \lambda}g_k^{*lk\ \gamma}g_q^{*\alpha l}\mathscr{W}_{\alpha jkl}(t)\hat{a}_k^{\dagger(\lambda)}\hat{b}_q^{\dagger(\gamma)}|0\,0\,a\rangle\ . \tag{2}$$

Here the sums over k and q are over the frequencies of the generated photons. The λ and γ sums are over horizontal and vertical polarization. The j,k,l sums are over all the intermediate Zeeman structure. The expression in Eqs. (2) is sum of all terms formed by stepping around the diamond, following the selection rules for the appropriate polarization, and weighting each term by the appropriate Clebsh-Gordan coefficients. The $\mathscr{W}_{\alpha jkl}(t)$ factor involves the four time integrals of the fourth order term in the Dyson's Series which after integration has the form $1/\delta_1\delta_2\delta_3\delta_4$ where the δ_i are various detunings which are the same for every term up to hyperfine splittings. We assume that the pairs we observe are far from intermediate resonance compared to the respective hyperfine splittings. Under this assumption we may pull the $\mathscr{W}_{\alpha jkl}(t)$

#148821 - $15.00 USD Received 7 Jun 2011; revised 2 Jul 2011; accepted 3 Jul 2011; published 14 Jul 2011

through the j,k,l and λ,γ sums. Since the measurements we make do not depend on frequency we can, for our current purpose, ignore the sums over k and q. Then the answer for a single initial sub-state is

$$|\psi_\alpha\rangle = \cos(\chi_\alpha)\,|HH\rangle + \sin(\chi_\alpha)\,|VV\rangle \ , \tag{3}$$

where $\cos(\chi_\alpha) \propto \sum_{j,k,l} \Omega_1^{j\alpha}\Omega_2^{k,j\ H} g_k^{*lk\ H} g_q^{*\alpha l}$. A similar equation exists for $\sin(\chi_\alpha)$ with H replaced by V. The coefficient for the HV and VH terms are zero for two horizontally polarized pumps. To take into account all of the Zeeman ground states as in Fig. 3C, we assume that the atoms begin in an incoherent mixture and the resulting state must be described by a density matrix $\rho = \sum_\alpha p_\alpha |\psi_\alpha\rangle\langle\psi_\alpha|$. The solution, after summing over all paths under the detuning condition, is the same regardless of the initial Zeeman state. It is $\cos(\chi_\alpha) = \sin(\chi_\alpha) = 1/\sqrt{2}$.

4. Autocorrelations

This system is also a source of heralded single photons (HSP). We use a the arrival of 780-nm signal photon to announce or herald the existence of a 1367-nm idler photon in the fiber. A common measure of the single-photon nature of the idler is the conditional autocorrelation at zero delay or

$$\tilde{g}^{(2)}(0) = \frac{\tilde{P}_{I1,I2}(0)}{\tilde{P}_{I1}\tilde{P}_{I2}} \ . \tag{4}$$

Here the tilde denotes conditional quantities. Thus, $\tilde{P}_{I1}$ and $\tilde{P}_{I2}$ are the probabilities that a count occurs in detector $I1$ and $I2$, respectively, given that a 780-nm photon has been detected. The conditional probability that both detectors register a count at the same time is given by $\tilde{P}_{I1,I2}(0)$. We expect $\tilde{g}^{(2)}(0) = 0$ for a perfect single photon state while a Poissonian source has $\tilde{g}^{(2)}(0) = 1$. Figure 4 shows the measured conditional autocorrelation function for different 795-nm pump powers. We see a decrease of coincidences of roughly a factor of twenty from a Poissonian source. At a pump power of 15 mW we observe $\tilde{g}^{(2)}(0) = 0.06(1)$, a heralding efficiency of 10% and a HSP generation rate of 1500 s^{-1} (detector and filter efficiency corrected). We have previously measured the bandwidth of the 1367-nm photons to be approximately 350 MHz [20]. The optical depth for resonant 780-nm photons is high at the operating temperature; the photon pairs generated near resonance are re-scattered and do not reach the detectors in the phase-matched direction. The photons that emerge from the cell are detuned from the intermediate resonance and this gives rise to the short correlation time larger bandwidth. Using a laser cooled sample Chaneliére *et al.* [8] have observed long N($>$ 15 ns) correlation times. Similar results for the conditional correlation through 4WM in a cooled fiber at 1.5 μm appear in Ref. [23].

Recent work in an all-fiber source of HSPs at 1570 nm with a photonic crystal through spontaneous four-wave mixing [12] demonstrated a rate of 9.2×10^4 heralded photons per second, and a high heralding efficiency of 52 % with a counts-to-accidentals ratio of 10.4. Narrowband filtering of the idler achieved a near time-bandwidth limited with a coherence length of 4 ps. This yields a HSP rate of 0.34 photons/s/MHz. In contrast, our atomic generation method, although producing fewer photons per second, has a rate of 4.3 photons/s/MHz, a substantially spectrally brighter source.

Figure 5 shows the observed autocorrelation of the 780-nm light field at two different temperatures of the cell. We use a time-stamper card and record arrival times for photons in detector $S1$ and $S2$ since the detectors are free running. The correlation function is then calculated off-line. We observe bunching in the $\tilde{g}_S^{(2)}(0)$ for the case of low optical depth (cell temperature of 347 K). At our typical operating temperature of 388 K, the autocorrelation function appears to be flat, within the experimental uncertainty. In an optically thick medium, multiple scattering events cause frequency redistribution of the photons across the entire Doppler width, leading

#148821 - $15.00 USD Received 7 Jun 2011; revised 2 Jul 2011; accepted 3 Jul 2011; published 14 Jul 2011

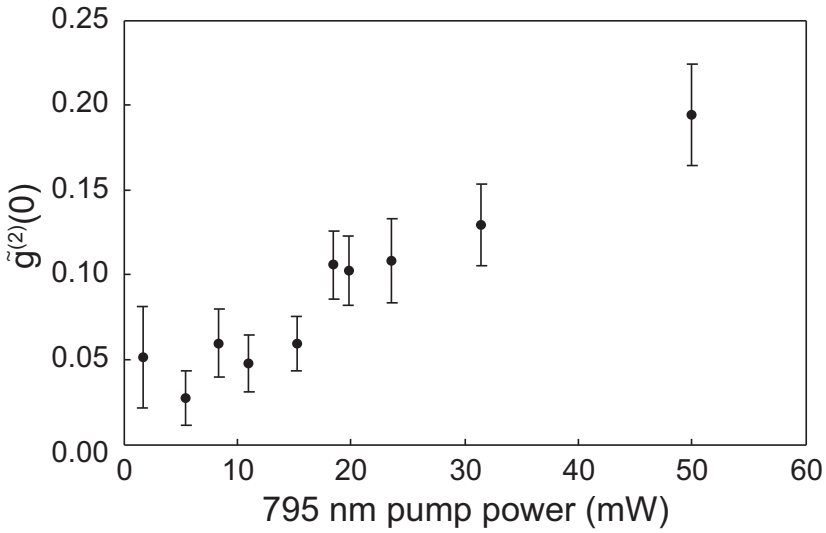

Fig. 4. Autocorrelation function for the 1367 nm light field conditioned on the arrival of a 780 nm photon.

to a very narrow autocorrelation [24]. At the 1-ns resolution used for all of our measurements here $g_S^{(2)}(0) = 1.0 \pm 0.1$, suggesting a correlation time much less than one ns.

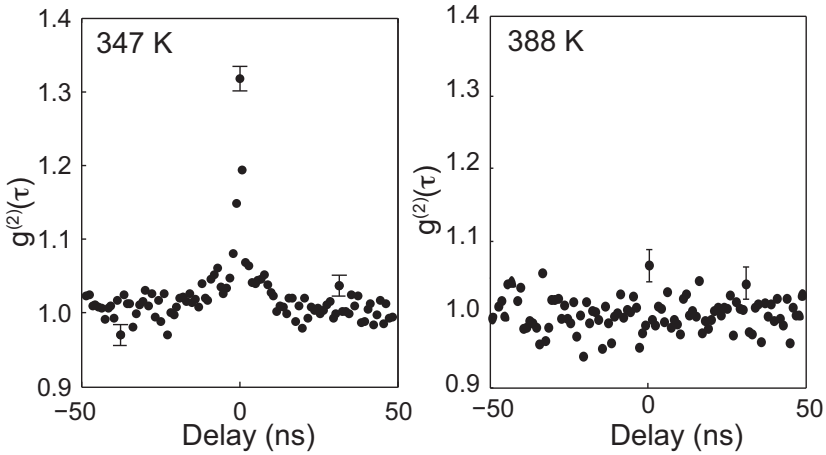

Fig. 5. The normalized autocorrelation function of the 780-nm light field at two different temperatures.

Figure 6 shows the autocorrelation function for the 1367-nm light field under the same pumping conditions indicated above. The measurement is performed by triggering both InGaAs APDs with a fixed delay between them at 7 MHz for 30 minutes per point. The output of the detectors is analyzed with a Field Programmable Gate Array (FPGA) circuit which records the number of singles and coincidences from detectors $I1$ and $I2$. The delay is changed by adding different lengths of coaxial cable between the triggering source and the detectors. We see that the light is bunched, as expected from light generated by a spontaneous process (the sample is optically thin at 1367 nm unlike at 780 nm). For a single polarization ther-

#148821 - $15.00 USD Received 7 Jun 2011; revised 2 Jul 2011; accepted 3 Jul 2011; published 14 Jul 2011

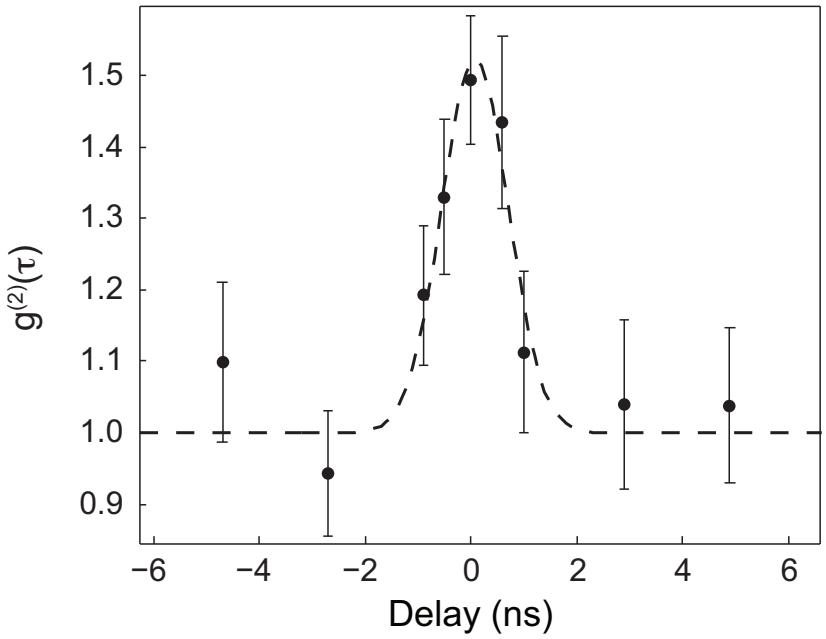

Fig. 6. Normalized autocorrelation function of the 1367 nm light field.

mal source $g_I^{(2)}(0) = 2$ [25], while for no polarization selection $g_I^{(2)}(0) = 1.5$. We measure $g_I^{(2)}(0) = 1.5 \pm 0.1$ consistent with our lack of polarization selection.

5. Cross-correlations

We measure the cross correlation function (CCF) of the photon pairs $g^{(2)}_{\rm cross}(\tau) = P_{I,S}(\tau)/(P_S P_I)$. Here P_S and P_I are the probabilities of receiving a count in any nanosecond time bin and $P_{I,S}(\tau)$ is the probability of detecting a signal and idler in two time bins separated by time τ. Figure 7 shows the unnormalized CCF, showing that the biphoton has a temporal profile of approximately one ns, in agreement with our previous measurements [20]. We see a peak raw coincidence rate of roughly 100 s^{-1} with an uncorrelated background of 5 s^{-1}. This ratio gives the maximum value of the normalized CCF to be $g^{(2)}_{\rm cross}(0) = 27.2 \pm 1.3$. Taking into account detector and filter efficiencies we observe a pair generation rate of 4,500 s^{-1}.

We combine these measurements in a version of the Cauchy-Schwarz inequality. Ref. [26] shows that for a two beam experiment for any classical field the correlation functions should satisfy:

$$R = \frac{\left[g^{(2)}_{\rm cross}(\tau)\right]^2}{g_S^{(2)}(0) g_I^{(2)}(0)} < 1\,. \tag{5}$$

We obtain a large violation with $R = 495 \pm 56$, demonstrating that the light at two very different wavelengths (780 nm and 1367 nm) is strongly non-classical. This violation with two different colors (780 nm and 1367 nm) is much larger than results found in other warm atom systems where the authors observed violations using the $D1$ (795 nm) and $D2$ (780 nm) lines of Rb with $R \approx 2$ [27]. Du and coworkers [7] reached R=11,000 in cold atoms, with the two beams almost degenerate around 780 nm.

#148821 - $15.00 USD Received 7 Jun 2011; revised 2 Jul 2011; accepted 3 Jul 2011; published 14 Jul 2011

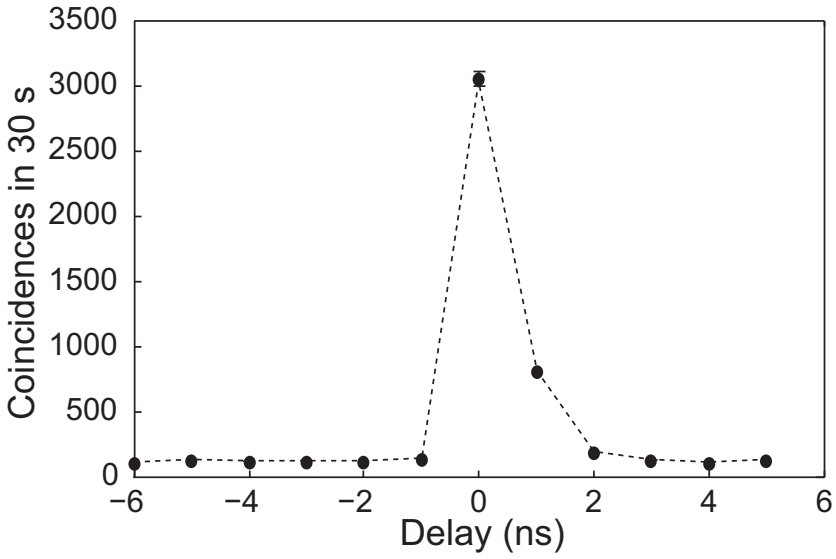

Fig. 7. The unnormalized cross-correlation function for the 780 nm and the 1367 nm fields showing the time correlation between them.

6. Conclusion

We have observed pair generation from a warm atomic ensemble at telecommunications and atomic memory compatible frequencies. We have measured an 8-σ violation of Bell's inequality, demonstrating the entanglement of the photons. The two fields, with different wavelengths (780 nm and 1367 nm), are highly non-classical as evidenced by a strong violation of the two beam Cauchy-Schwarz inequality. We have shown that the system can function as a narrow-band, heralded single-photon source with generation rates greater than 10^3 s^{-1}. This system, based on a simple vapor cell, thus produces both photons in the telecommunication band as well as narrow-band photons that can interact with atomic ensembles, suitable for application to quantum repeaters.

Acknowledgments

The authors thank David Norris for helpful conversations, Dzmitry Matsukevich for designing the FPGA system used for data acquisition, and Alan Migdall for the loan of an InGaAs APD. This work was supported by NSF, DURIP, and CONACYT.

#148821 - $15.00 USD Received 7 Jun 2011; revised 2 Jul 2011; accepted 3 Jul 2011; published 14 Jul 2011